Unusual Free Radical Polymerization of Vinyl Acetate in Anionic Microemulsion Media

N. Sosa, E. A. Zaragoza, R. G. López, and R. D. Peralta*

Centro de Investigación en Química Aplicada, Boulevard Ing. Enrique Reyna H. No. 140, Saltillo, Coahuila 25100, Mexico

I. Katime

Grupo de Nuevos Materiales, Departamento de Química Física, Universidad del País Vasco—Campus Leioa, Bilbao 48080, Spain

F. Becerra, E. Mendizábal, and J. E. Puig

Departamento de Ingeniería Química, Universidad de Guadalajara, Boulevard Marcelino García Barragán No. 1451, Guadalajara, Jal. 44430, Mexico

Received August 6, 1999. In Final Form: November 18, 1999

The polymerization of vinyl acetate in one-phase o/w microemulsions stabilized with Aerosol OT (AOT) is examined as a function of concentration and type of initiator (V-50 and KPS) and temperature. Conversions and reaction rates increase with increasing concentration of V-50 and temperature. Faster polymerization rates and higher conversions are achieved with KPS because of the different electrostatic interactions between the charged microemulsion droplets and the free radicals of KPS and V-50. Average molar masses and polydispersity indexes (M_w/M_n) are much smaller than those observed in emulsion polymerization using the same surfactant, even at high conversions. Analysis of the molar mass distribution indicates that chain-transfer reactions to monomer are the controlling chain-growth mechanism in the polymerization of vinyl acetate in AOT microemulsions at all conversions.

Introduction

Even though emulsion and microemulsion polymerization appear to be similar—both can produce colloidal polymer particles of high molar mass with fast reaction rates,[1−5] they are in fact entirely different from a kinetic point of view. Emulsion polymerization exhibits three reaction rate intervals (nucleation, propagation, and termination),[1,2] whereas only two rate intervals are detected in microemulsion polymerization.[5−12] Both homogeneous and micellar nucleation mechanisms can occur in microemulsion polymerization owing to the large amount of surfactant present, which also causes the continuous generation of particles,[5,7] whereas homogeneous nucleation is important only in the emulsion polymerization of polar monomers.[13] Moreover, both particle size and average number of chains per particle are considerably smaller in microemulsion polymerization.[5] A main drawback of microemulsion polymerization is the low ratio of polymer produced to surfactant employed. However, efforts to increase this ratio have been reported recently.[14−19]

The polymers produced by emulsion and microemulsion polymerization can also have different characteristics. For instance, a cross-linked poly(tetrahydrofurfuryl methacrylate) is produced by emulsion polymerization, whereas a branched polymer with a large molar mass (ca. 10^7 g/mol) is obtained in microemulsion polymerization.[6] Isotactic poly(methyl methacrylate) is produced by microemulsion polymerization, whereas the atactic form is obtained in emulsion polymerization.[20] Recently we reported that the polymerization of vinyl acetate (VA) stabilized with the cationic surfactant cetyltrimethylammonium bromide

* To whom correspondence should be addressed.

(1) Piirma, I. *Emulsion Polymerization*; Academic Press: New York, 1980.
(2) Gilbert, R. G. *Emulsion Polymerization. A Mechanistic Approach*; Academic Press: New York, 1995.
(3) Candau, F. In *Encyclopedia of Polymer Science and Engineering*; Mark, H. F., Bikales, N. M., Overberger, C. G., Menges, G., Eds.; Wiley: New York, 1987; Vol. 9.
(4) Dunn, A. S. In *Comprehensive Polymer Science*; Eastwood, G. C., Ledwith, A., Sigwalt, P., Eds.; Pergamon: New York, 1988; Vol. 4.
(5) Puig, J. E. In *Polymeric Materials Encyclopedia*; Salamone, J. C., Ed.; CRC Press: Boca Raton, FL, 1996; Vol. 6.
(6) Full, A. P.; Puig, J. E.; Gron, L. U.; Kaler, E. W.; Minter, J. R.; Mourey, T. H.; Texter, J. *Macromolecules* **1992**, *25*, 5157.
(7) Puig, J. E.; Pérez-Luna, V. H.; Pérez-González, M.; Macías, E. R.; Rodríguez, B. E.; Kaler, E. W. *Colloid Polym. Sci.* **1993**, *271*, 114.
(8) Rodríguez-Guadarrama, L. A.; Mendizábal, E.; Puig, J. E.; Kaler, E. W. *J. Appl. Polym. Sci.* **1993**, *48*, 775.
(9) Escalante-Vázquez, J. I.; Rodríguez-Guadarrama, L. A.; López, R. G.; Mendizábal, E.; Puig, J. E.; Katime, I. *J. Appl. Polym. Sci.* **1996**, *62*, 1313.
(10) Bleger, F.; Murthy, A. K.; Pla, F.; Kaler, E. W. *Macromolecules* **1994**, *27*, 2559.
(11) Full, A. P.; Kaler, E. W.; Arellano, J.; Puig, J. E. *Macromolecules* **1996**, *29*, 2764.
(12) Morgan, J. D.; Lusvardi, K. M.; Kaler, E. W. *Macromolecules* **1997**, *30*, 1897.
(13) Eliseeva, V. I.; Ivanchev, S. S.; Kuchanov, S. I.; Lebedev, A. V. *Emulsion Polymerization and Its Applications in Industry*; Consultants Bureau: New York, 1981.
(14) Gan, L. M.; Lian, N.; Chew, C. H.; Ng, S. C. *Langmuir* **1994**, *10*, 2197.
(15) Loh, S. E.; Gan, L. M.; Chew, C. H.; Ng, S. C. *J. Macromol. Sci., Pure Appl. Chem.* **1996**, *A33*, 371.
(16) Rabelero, M.; Zacarías, M.; Mendizábal, E.; Puig, J. E.; Domínguez, J. M. *Polym. Bull.* **1997**, *38*, 695.
(17) Xu, X.; Zhang, Z.; Wu, H.; Ge, X.; Zhang, M. *Polymer* **1998**, *39*, 5245.
(18) Ming, W.; Jones, F. N.; Fu, S. *Polym. Bull.* **1998**, *40*, 749.
(19) Ming, W.; Jones, F. N.; Fu, S. *Macromol. Chem. Phys.* **1998**, *199*, 1075.
(20) Roy, S.; Devi, S. *J. Appl. Polym. Sci.* **1996**, *62*, 1509.

10.1021/la991065m CCC: $19.00
Published on Web 03/25/2000

(CTAB) yielded a polymer with a molar mass distribution (MMD) controlled mostly by chain-transfer reactions to monomer *even* at high conversions—although termination by chain transfer to polymer was also evident.[21,22] By contrast, the emulsion polymerization of this monomer produced a highly branched polymer of large molar mass and broad MMD because chain transfer to polymer is the controlling mechanism for chain growth and termination, particularly at high conversions.[23−26]

By far, the monomers most extensively studied by microemulsion polymerization are styrene and methyl methacrylate.[7,8,10−12,27−33] The microemulsion polymerization of more polar monomers, such as VA, has been scarcely studied.[21,22,34−36] It is noteworthy to mention the work of Donescu et al., who polymerized VA in cosolubilized systems made of surfactant, cosurfactant, water, and VA.[37, 38]

Here the polymerization of VA in three-component microemulsions stabilized with small amounts of Aerosol OT (1 wt %) is presented as a function of type and concentration of initiator and temperature. VA was also polymerized in emulsions stabilized with Aerosol OT using the same initiators to compare the kinetics of the polymerization as well as the characteristics of the latexes and polymers produced by these two processes.

Experimental Section

Sodium bis(2-ethylhexyl)sulfosuccinate (Aerosol OT or AOT) was 98% pure from Fluka. It was dried and stored in a desiccator jar prior to use. VA (Aldrich) was distilled at 30 °C under reduced pressure and argon atmosphere, stored at 4 °C in dark vials, and used within 30 h after distillation. 2,2′-Azobis(2-amidinopropane) dihydrochloride (V-50) from Wako Chem. was recrystallized from methanol. Potassium persulfate (KPS) and hydroquinone were 99% pure from Aldrich, and they were used as received. Water was doubly distilled and deionized.

The one-phase microemulsion regions (o/w and w/o) were determined by titration of AOT/water solutions with VA and by titration of AOT/VA solutions with water. Phase boundaries were detected visually at each constant AOT/water or AOT/VA line. Then, samples with compositions slightly below and above the visually determined phase boundaries were prepared by weighing each component and allowed to reach equilibrium in a water bath at either 25 or 60 °C to determine more precisely the phase boundaries. Clear samples that did not exhibit static or streaming birefringence when examined through cross polarizers were considered one-phase microemulsions. The lamellar phase was identified by its texture in polarizing microscopy; however, its boundaries were not determined accurately. The phase diagram at high AOT concentrations was not examined since it is not relevant for the present paper. Electrical conductivities were measured with an Orion 101 conductimeter at 60 °C and 1000 Hz.

A 100 mL glass reactor with magnetic stirring was employed to polymerize microemulsions made along an AOT/H_2O ratio of 1/99 (w/w) and 3 wt % VA. The concentrations of V-50 and KPS are reported in mole fraction with respect to monomer content. Prior to polymerization, VA and the AOT aqueous solution were degassed by cooling, pumping, and heating cycles. The reacting system was continuously stirred and purged with argon during the entire reaction. Conversion was followed by gravimetry: samples were withdrawn from the reacting system at given times and put in vials (of known weight) immersed in an ice bath containing 0.5 g of a hydroquinone solution (0.4%). Samples were then weighed and freeze-dried. The weight of polymer was estimated by subtracting the known weights of AOT and hydroquinone from the total weight of the freeze-dried sample.

Particle size was measured in a Malvern 4700 quasielastic light-scattering (QLS) apparatus equipped with an argon laser ($\lambda = 488$ nm). Measurements were performed at 25 °C and at an angle of 90°. Intensity correlation data were analyzed by the method of cumulants to provide the average decay rate, $\langle\Gamma^2\rangle$ ($=q^2D$), where $q = (4\pi n/\lambda)\sin(\theta/2)$ is the scattering vector, n the index of refraction, and D the diffusion coefficient. The measured diffusion coefficients were represented in terms of apparent diameters by means of Stokes law assuming that the solvent has the viscosity of water. Latexes were diluted up to 100 times and filtered through 0.2 μm Millipore filters before QLS measurements to minimize particle−particle interactions and to remove dust particles.

Freeze-dried samples for gel permeation chromatography (GPC) were washed with hot water to remove most AOT. The dried polymer (and the remaining AOT) were dissolved in acetone at 40 °C and centrifuged at 14 000 rpm and 5 °C for 25 min to separate the AOT. The supernatant was extracted with a pipet, the acetone evaporated, and the polymer dissolved in HPLC-grade tetrahydrofurane (Merck), used as the mobile phase. Average molar masses and molar mass distributions (MMD) were measured with a LC30 Perkin-Elmer gel permeation chromatograph equipped with a refractive index and Dawn multiangle light-scattering detectors.

Results

Phase Behavior. Phase diagrams of AOT/water/VA at 25 and 60 °C are shown in Figure 1. At 25 °C, the one-phase o/w microemulsion region (L_1) is small and protrudes as a tongue from the water-rich corner. The w/o one-phase microemulsion region (L_2), in contrast, is large and extends to more than 60 wt % VA toward the water-rich corner. Between the L_1 and L_2 regions, there is an ample emulsion region, which also shares a phase boundary with the lamellar region (L_α). At 60 °C, the microemulsion region spans continuously from the water side to the oil side of the phase diagram. The emulsion region has split in two and shrunk whereas the L_α region increases as the temperature is raised from 25 to 60 °C.

The electrical conductivity is high (a few mS/cm) in the o/w microemulsion region. In this region, conductivity increases rapidly with increasing Aerosol OT content and slightly with increasing VA content (Table 1). By contrast, conductivity is low (a few μS/cm) in the w/o microemulsion region (Table 2). Conductivity increases with increasing water content along constant AOT/VA lines. At a water content of 60 wt % in the 25/75 AOT/VA line, the conductivity is larger than 7×10^3 μS/cm, which is similar

(21) López, R. G.; Treviño, M. E.; Salazar, L. V.; Peralta, R. D.; Becerra, F.; Puig, J. E.; Mendizábal, E. *Polym. Bull.* **1997**, *38*, 411.
(22) López, R. G.; Treviño, M. E.; Peralta, R. D.; Katime, I.; Flores, J.; Becerra, F.; Mendizábal, E.; Puig, J. E. *Macromolecules*, in press.
(23) Friis, N.; Hamielec, A. E. *J. Appl. Polym. Sci.* **1975**, *19*, 97.
(24) El-Aasser, M. S.; Makgawinata, T.; Vanderhoff, J. W.; Pichot, C. *J. Polym. Sci., Polym. Chem. Ed.* **1983**, *21*, 2363.
(25) Tobita, H. *Polymer* **1994**, *35*, 3023.
(26) Vandezande, G. A.; Smith, O. W.; Bassett, D. R. In *Emulsion Polymerization and Emulsion Polymers*; Lovell, P. A., El-Aasser, M. S., Eds.; Academic Press: New York, 1997; pp 564−587.
(27) Kuo, P. L.; Turro, N. J.; Tseng, C.; El-Aasser, M. S.; Vanderhoff, J. W. *Macromolecules* **1987**, *20*, 1216.
(28) Guo, J. S.; El-Aasser, M. S.; Vanderhoff, J. W. *J. Polym. Sci., Polym. Chem. Ed.* **1989**, *27*, 691.
(29) Pérez-Luna, V. H.; Puig, J. E.; Castaño, V. M.; Rodríguez, B. E.; Murthy, A. K.; Kaler, E. W. *Langmuir* **1990**, *6*, 1040.
(30) Feng, L.; Ng, K. Y. *Macromolecules* **1990**, *23*, 1048.
(31) Antonietti, M.; Bremser, S.; Müschenborn, D.; Rosenauer, C.; Schupp, B.; Schmidt, M. *Macromolecules* **1991**, *24*, 6636.
(32) Gan, L. M.; Chew, C. H.; Lye, I.; Imae, T. *Polym. Bull.* **1991**, *25*, 193.
(33) Gan, L. M.; Chew, C. H.; Ng, S. C.; Loh, S. E. *Langmuir* **1993**, *9*, 2799.
(34) Nikitina, S. A.; Spiridonova, V. A.; Taubmann, A. B. *J. Polym. Sci., Polym. Chem. Ed.* **1970**, *8*, 3045.
(35) Treviño, M. E.; López, R. G.; Peralta, R. D.; Becerra, F.; Mendizábal, E.; Puig, J. E. *Polym. Bull.* **1999**, *42*, 411.
(36) Sosa, N.; López, R. G.; Peralta, R. D.; Katime, I.; Becerra, F.; Mendizábal, E.; Puig, J. E. *Macromol. Chem. Phys.* **1999**, *200*, 2416.
(37) Donescu, D.; Anghel, D. F.; Balcan, M. *Angew Makromol. Chem.* **1990**, *175*, 1.
(38) Donescu, D.; Anghel, D. F.; Gosa, K.; Balcan, M. *Angew Makromol. Chem.* **1991**, *188*, 1.

Table 1. Electrical Conductivity at 60 °C of Microemulsions Made Along Constant AOT/H_2O Lines as a Function of VA Content

AOT/water = 1/99		AOT/water = 4/96		AOT/water = 7/93		AOT/water = 12/88	
VA (wt %)	*k* (mS/cm)	VA (wt %)	*k* (mS/cm)	VA (wt %)	*k* (mS/cm)	VA (wt %)	*k* (mS/cm)
0	1.47	0	3.54	7.2	6.4	20.8	7.81
0.91	1.47	2.0	4.45	8.7	6.3	21.7	7.74
2.3	1.45	3.5	4.5	10	6.2	23.3	7.78
2.9	1.46	4.6	4.99				
3.5	1.46						

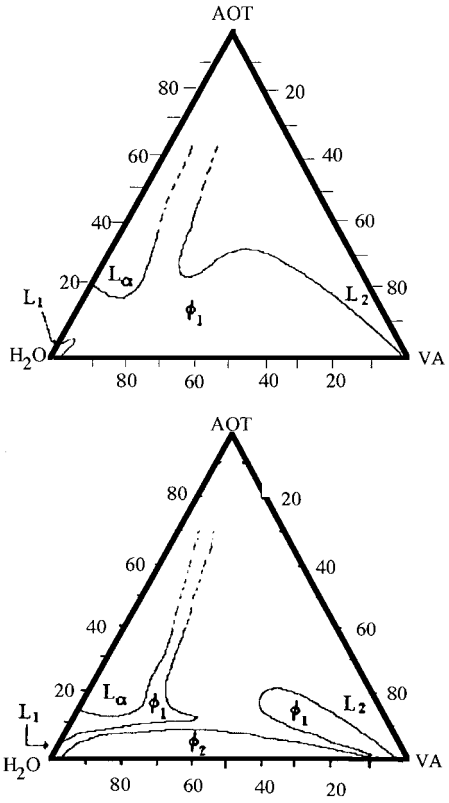

Figure 1. Phase diagram of Aerosol OT, water, and vinyl acetate at 25 °C (A, top) and 60 °C (B, bottom).

Table 2. Electrical Conductivity at 60 °C of Microemulsions Made Along Constant AOT/VA Lines as a Function of H_2O Content

AOT/VA = 15/85		AOT/VA = 25/75	
H_2O (wt %)	*k* (μS/cm)	H_2O (wt %)	*k* (μS/cm)
0	1	0	3.1
10.7	19.9	19.6	63.6
20	29.6	35.2	200
26.8	66.1	45.1	1700
32.5	300	60	7340

to that observed in the L_1 region (cf. Tables 1 and 2). Nearby, along the 12/88 AOT/water line at a VA content of 23%, conductivity is also of the same order of magnitude.

Kinetics. Figure 2A reports conversion as a function of time for the polymerization of VA in AOT microemulsions initiated at 60 °C with different V-50 concentrations. Both conversion and reaction rate increase with increasing V-50 concentration. Plots of polymerization rate as a function of conversion reveal only two rate intervals; moreover, the maximum reaction rate (R_{pmax}) is detected at the same conversion ($x_{max} \approx 19\%$) regardless of the level of initiator concentration (Figure 2B). From a double-logarithm plot of R_{pmax} versus initiator concentration, a power law correlation of the form $R_{pmax} \propto [\text{V-50}]^{0.8}$ was found.

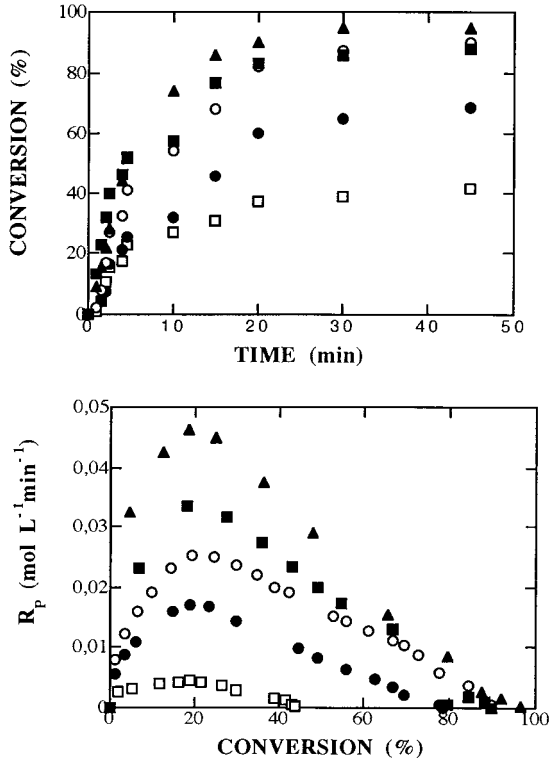

Figure 2. (A, top) Conversion versus time for the polymerization of vinyl acetate in AOT microemulsions (3 wt % VA, 0.97 wt % AOT, and 96.03 wt % H_2O) initiated at 60 °C with different V-50 concentrations (n_{V-50}/n_{VA}): (□) 3.17×10^{-4}; (●) 9.51×10^{-4}; (○) 2.06×10^{-3}; (■) 3.17×10^{-3}; (▲) 4.8×10^{-3}. (B, bottom) Reaction rate versus conversion for data shown in Figure 2A.

The effect of temperature on conversion and reaction rate is depicted in Figure 3 for the polymerization of VA initiated with V-50 ($n_{V-50}/n_{VA} = 3.17 \times 10^{-3}$). Both conversion and reaction rate increase as the reaction temperature is raised. Again, only two reaction rate intervals are observed (Figure 3B). Notice that x_{max} shifts slightly to lower values upon increasing temperature. A plot of the logarithm of R_{pmax} versus the reciprocal of the absolute temperature (not shown) gives a straight line indicating an Arrhenius behavior. From the slope of this plot, an activation energy (E_a) of 82.4 kJ/mol was estimated.

Polymerization was also carried out with KPS because this initiator decomposes into anionic free radicals in contrast to V-50 that yields cationic free radicals. Figure 4A shows conversion as a function of time for the polymerization of VA initiated with KPS ($n_{KPS}/n_{VA} = 3.2 \times 10^{-3}$) at 60 °C. Also, for comparison, conversion versus time data are included in this figure for the polymerization of VA in a microemulsion of identical composition but initiated with V-50 ($n_{V-50}/n_{VA} = 3.17 \times 10^{-4}$) at 60 °C. The concentrations of V-50 and KPS were chosen to produce equal fluxes of free radicals since V-50 decomposes 10

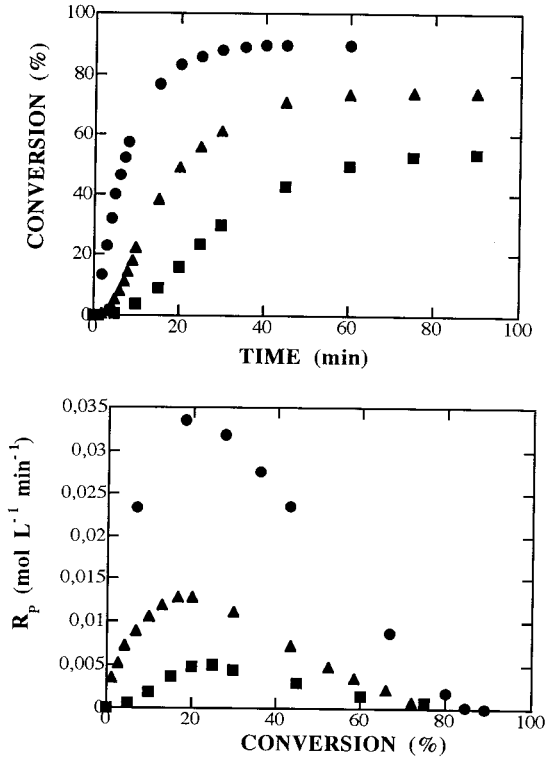

Figure 3. (A, top) Conversion versus time for the polymerization of vinyl acetate in AOT microemulsions (3 wt % VA, 0.97 wt % AOT, and 96.03 wt % H_2O) initiated with V-50 (3.17×10^{-3}) at different temperatures: (■) 40 °C; (▲) 50 °C; (●) 60 °C. (B, bottom) Reaction rate versus conversion for data shown in Figure 3A.

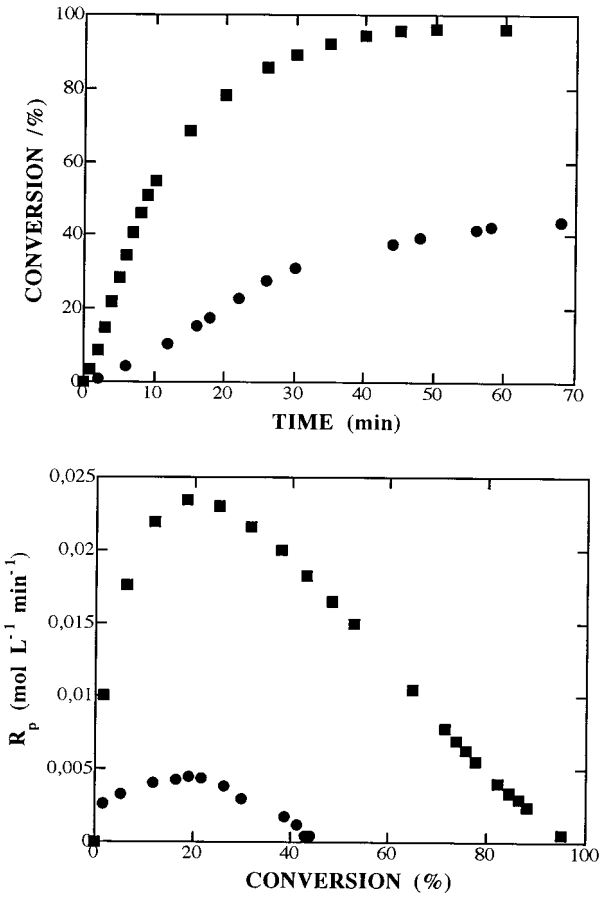

Figure 4. (A, top) Conversion versus time for the polymerization of vinyl acetate in AOT microemulsions (3 wt % VA, 0.97 wt % AOT and 96.03 wt % H_2O) initiated with V-50 (●) or KPS (■) at 60 °C. The concentrations of KPS (3.17×10^{-3}) and V-50 (3.17×10^{-4}) were chosen to yield equal fluxes of free radicals. (B, bottom) Reaction rate versus conversion for data shown in Figure 4A.

times faster than KPS at 60 °C. At this temperature, the decomposition rate constant (k_d) of V-50 is 3.2×10^{-5} s^{-1} according to the manufacturer whereas that of KPS is 3.1×10^{-6} s^{-1}.[39] Faster reaction rates and higher conversions are achieved with KPS—conversion is near 100% with KPS after 50 min of reaction whereas conversion does not exceed 50% with V-50 in the same period of time (Figure 4A). Reaction rate as a function of conversion discloses again two rate intervals with both initiators (Figure 4B). R_{pmax} is nearly five times larger with KPS than with V-50. However, x_{max} is practically the same (ca. 19%) with both initiators.

VA was also polymerized in emulsion media (AOT/H_2O ratio of 1/99 by weight and 10 wt % VA) initiated at 60 °C with V-50 ($n_{V-50}/n_{VA} = 3.17 \times 10^{-4}$) or KPS ($n_{KPS}/n_{VA} = 3.2 \times 10^{-3}$) to compare the kinetic schemes and the reaction mechanisms of emulsion and microemulsion polymerization. Figure 5 shows plots of conversion versus time and of reaction rate as a function of conversion. Conversions are higher and reaction rates are faster again with KPS. Moreover, three reaction rate intervals are clearly defined with an intermediate constant-reaction-rate interval, which corresponds to the propagation step (Figure 5B). Notice that the reaction rate in the propagation step is about six times larger than R_{pmax} in microemulsion polymerization for KPS and nearly 10 times larger for V-50 (cf. Figures 4B and 5B).

Latex Characterization. Table 3 reports the average-number molar mass ($\bar{M}_n$), the polydispersity index ($\bar{M}_w/\bar{M}_n$), and the latex particle size (D_p) as a function of V-50 concentration at final conversions (Figure 2A). Molar masses and $\bar{M}_w/\bar{M}_n$ are quite insensitive to the level of initiator concentration employed. Moreover, they are much smaller than typical values reported for emulsion polymerization of this monomer.[23−26] On the other hand, particle size increases slightly upon increasing initiator concentration. The number density of particles, N_p, estimated from conversion and with the assumption that all particles have a size equal to D_p, is around 3×10^{15} mL^{-1}. Likewise, with the assumption that all polymer chains have a molar mass equal to $\bar{M}_n$, an average number of chains per particle, N_c, was estimated to be between 6 and 25, depending on initiator concentration. These values are much smaller than those typically found in emulsion polymerization.[1,2]

$\bar{M}_n$, $\bar{M}_w/\bar{M}_n$, and D_p for the polymerization of the VA microemulsions initiated with V-50 ($n_{V-50}/n_{VA} = 3.17 \times 10^{-3}$) at different temperatures are shown in Table 4. Values of $\bar{M}_n$ and $\bar{M}_w/\bar{M}_n$ do not seem to depend on temperature, and, again, they are much smaller than values reported for the emulsion polymerization of this monomer.[23−26] Particle size, in turn, increases with decreasing reaction temperature.

Values of $\bar{M}_n$, $\bar{M}_w/\bar{M}_n$, and D_p at various conversions for the polymerization of VA in AOT microemulsions initiated at 60 °C with V-50 ($n_{V-50}/n_{VA} = 3.17 \times 10^{-3}$) or with KPS ($n_{V-50}/n_{VA} = 3.20 \times 10^{-3}$) are reported in Table 5. With both initiators, $\bar{M}_n$ increases slightly with conversion but $\bar{M}_w/\bar{M}_n$ is about the same at all conversions. Particle size remains fairly constant throughout the reaction, except

(39) Brandrup, J.; Immergut, E. H.; Grulke, E. A. *Polymer Handbook*; Wiley: New York, 1999.

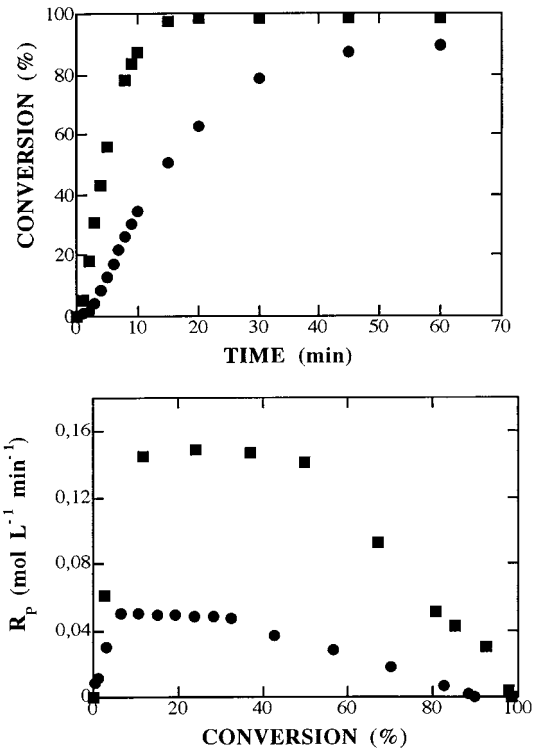

Figure 5. (A, top) Conversion versus time for the polymerization of vinyl acetate in AOT emulsions (10 wt % VA, 0.90 wt % AOT, and 89.1 wt % H_2O) initiated with V-50 (●) or KPS (■) at 60 °C. The concentrations of KPS (3.17×10^{-3}) and V-50 (3.17×10^{-4}) were chosen to yield equal fluxes of free radicals. (B, bottom) Reaction rate versus conversion for data shown in Figure 5A.

Table 3. Average-Number Molar Mass, Polydispersity Index, and Particle Size of Poly(vinyl acetate) Obtained at the End (according to Figure 2) of the Microemulsion Polymerization with Various V-50 Concentrations

[V-50] × 10^3 (n_{V-50}/n_{VA})	$\bar{M}_n \times 10^{-5}$ (g/mol)	$\bar{M}_w/\bar{M}_n$	D_p (nm)
0.317	4.3	1.4	25.5
0.95	2.4	2.3	26.6
2.06	2.6	2.4	26.7
3.17	5.3	1.6	29.6
4.76	4.6	1.5	31.0

Table 4. Average-Number Molar Mass, Polydispersity Index, and Particle Size of Poly(vinyl acetate) Obtained after 90 min of Polymerization (see Figure 3) as a Function of Temperature of Reaction

T (°C)	conversion (%)	$\bar{M}_n \times 10^{-5}$ (g/mol)	$\bar{M}_w/\bar{M}_n$	D_p (nm)
40	55.0	4.6	1.6	
50	72.0	3.7	1.8	43
60	87.0	5.3	1.6	30

at the highest conversion with KPS, where larger particles are detected.

Table 6 depicts values of $\bar{M}_n$, $\bar{M}_w/\bar{M}_n$, and D_p at different conversions for the emulsion polymerization of this monomer initiated at 60 °C with KPS or V-50. $\bar{M}_n$, $\bar{M}_w/\bar{M}_n$, and D_p change with conversion very differently than those reported for microemulsion polymerization (Table 5). At low conversions, values of $\bar{M}_n$ and $\bar{M}_w/\bar{M}_n$ are similar to those found in microemulsion polymerization; however, as conversion increases, both $\bar{M}_n$ and $\bar{M}_w/\bar{M}_n$ augment and become substantially larger than those obtained in microemulsion polymerization under similar reaction conditions and conversions (cf. Tables 5 and 6). Particles are larger in emulsion polymerization, even at low conversions, and grow with conversion. Final particle size with both initiators is much larger than those obtained by microemulsion polymerization (cf. Tables 5 and 6).

Discussion and Conclusions

The double-tail anionic surfactant, Aerosol OT, usually does not form o/w microemulsions with oils because of its large effective surfactant parameter, $v/(a_0 l_c)$, where v is the volume of the hydrocarbon tails, a_0 the area of the polar head at the interface, and l_c the length of the extended hydrocarbon tails.[40] However, with polar monomers such as MMA, *N*-methylolacrylamide (NMA), and tetrahydrofurfuryl methacrylate (THFM), AOT does form one-phase o/w microemulsions because these polar monomers act as cosurfactants and place themselves at the interface.[6,8,41] With VA, Aerosol OT also forms transparent, fluid, and highly conductive one-phase samples at 25 and 60 °C near the water-rich corner of the phase diagram (Figure 1). Evidently, similar to MMA, NMA, and THFM, some VA molecules go to the interface and there, together with the AOT molecules, produce the necessary curvature to allow the formation of o/w microemulsions. The transparency, low viscosity, composition, and high conductivity (Table 1) confirm water-continuous microstructures, i.e., o/w microemulsions. Conductivity increases with increasing AOT/water ratio as expected (Table 1). However, in contrast to the behavior observed with styrene and other monomers,[7,9] conductivity raises slightly upon increasing VA content. This behavior, also reported for methyl methacrylate (MMA) microemulsions[8] and for VA microemulsions stabilized with CTAB,[21] has been attributed to the partial hydrolysis of these monomers. This effect must be important enough to overcome the decrease in conductivity produced by micellar growth upon incorporation of monomer.

In the L_2 region, samples are transparent, fluid, but poorly conductive (Table 2), demonstrating the existence of a w/o microemulsion structure, which is typical of Aerosol OT. Upon increasing the temperature from 25 to 60 °C, the L_1 and the L_2 regions merge together. At water/oil ratios close to one, samples are slightly bluish, fluid, and highly conductive (Table 2), which may indicate the formation of bicontinuous microemulsions. However, further tests are needed to demonstrate the existence of this structure.

The initially transparent o/w microemulsions become slightly bluish at the onset of polymerization and increasingly turbid as the reaction proceeds because of particle growth and the increasing refractive index contrast between particles and the aqueous medium as monomer changes into polymer. Final latexes are bluish and opaque; also, they have not shown signs of coagulation after a few months of storage at room temperature. Polymerization of VA in Aerosol OT microemulsions is fast, and the polymerization rates increase with increasing V-50 concentration (Figure 2) and temperature (Figure 3). An increase in initiator concentration yields faster reactions owing to the larger flux of free radicals, which produces a higher probability of both homogeneous and micellar nucleation of particles. Increasing the temperature of reaction results in faster reaction rates and higher conversions because of the increase in the V-50 decomposition rate constant and the VA propagation rate

(40) Mitchel, D. J.; Ninham, B. W. *J. Chem. Soc., Faraday Trans 2* **1981**, *77*, 601.
(41) Macías, E. R.; Rodríguez-Guadarrama, L. A.; Cisneros, B. A.; Castañeda, A.; Mendizábal, E.; Puig, J. E. *Colloids Surf. A* **1995**, *103*, 119.

Table 5. Average-number Molar Mass, Polydispersity Index, and Particle Size Measured at Various Conversions for the Microemulsion Polymerization of VA Initiated at 60 °C with KPS ($n_{KPS}/n_{VA} = 3.2 \times 10^{-3}$) or V-50 ($n_{V-50}/n_{VA} = 3.17 \times 10^{-3}$)

KPS				V-50			
conversion (%)	$\bar{M}_n \times 10^{-5}$ (g/mol)	$\bar{M}_w/\bar{M}_n$	D_p (nm)	conversion (%)	$\bar{M}_n \times 10^{-5}$ (g/mol)	$\bar{M}_w/\bar{M}_n$	D_p (nm)
28.5	2.7	1.7	21.5	33.4	2.8	1.7	36
36.7	3.4	1.6	21.5	58.7	3.7	1.5	30
49.6	2.8	2.1	22.1	86.4	5.3	1.6	30
97.1	5.1	1.8	33.3				

Table 6. Average-Number Molar Mass, Polydispersity Index, and Particle Size Measured at Various Conversions for the Emulsion Polymerization of VA Initiated at 60 °C with KPS ($n_{KPS}/n_{VA} = 3.2 \times 10^{-3}$) or V-50 ($n_{V-50}/n_{VA} = 3.17 \times 10^{-4}$)

KPS				V-50			
conversion (%)	$\bar{M}_n \times 10^{-5}$ (g/mol)	$\bar{M}_w/\bar{M}_n$	D_p (nm)	conversion (%)	$\bar{M}_n \times 10^{-5}$ (g/mol)	$\bar{M}_w/\bar{M}_n$	D_p (nm)
7.0	5.5	1.2		24.5	7.5	1.4	70
35.5	7.5	1.4		51.0	8.9	1.8	86
58.0	8.8	1.6	63	93.0	9.3	4.0	100
74.7	12.5	1.9	71				
97.0	20.9	2.1	80				

constant. Moreover, since the solubility of VA in water increases with increasing temperature, the contribution of homogeneous nucleation may be more important.

Only two reaction rate intervals are detected at all V-50 concentrations (Figure 2B), all temperatures (Figure 3B), and for both KPS and V-50 (Figure 4B). The polymerization rate first increases rapidly because of the fast particle nucleation rate, and then it decreases steadily after passing through a maximum, because monomer concentration within the particles begins to diminish as a result of the disappearance of the microemulsion droplets and/or the monomer dissolved in the aqueous phase—the latter fact is important in the polymerization of more water-soluble monomers such as VA. This does not contravene the continuous particle nucleation mechanism that has been proposed for microemulsion polymerization.[5,10,28] In fact, the large amount of surfactant present in microemulsion polymerization allows the nucleation and stabilization of new particles throughout the reaction.

The maximum reaction rate is detected at about the same conversion ($x_{max} \approx 19 \pm 1\%$) regardless of the type and concentration of initiator and temperature, although, at 40 °C, it shifts slightly to higher values (Figure 3B) probably because of a change in the water solubility of VA or experimental (or numerical) uncertainties. The same value of x_{max} was reported for the polymerization of VA in ternary microemulsions stabilized with CTAB.[21,22] However, for the polymerization of VA in microemulsions stabilized with a mixture of dodecyltrimethylammonium bromide (DTAB) and didodecyldimethylammonium bromide (DDAB), x_{max} was detected at higher conversions (ca. 25%).[35] For other systems, x_{max} does not change with changes in monomer and initiator concentrations, but it varies from monomer to monomer. For instance, x_{max} is 20% for styrene, 32% for methyl methacrylate, 30% for *n*-butyl methacrylate, and 39% for *n*-hexyl methacrylate.[7−9,12,42,43]

In emulsion polymerization, reaction rate slows down when the number of particles becomes constant and the monomer concentration (and/or the average number of free radicals per particle) decreases.[1,2] In microemulsion polymerization the explanation of the maximum in reaction rate is more complicated inasmuch as particles are generated throughout the reaction.[10,43] Guo et al. suggested that the interval *I* in microemulsion polymerization (of styrene) ends when all the microemulsion droplets have disappeared either by becoming polymer particles or by being consumed by diffusion of their monomer to the reacting particles; then reaction rate diminishes because monomer concentration in the particles decreases.[28] Mendizábal et al. have suggested the same mechanism for the microemulsion polymerization of water-insoluble monomers (i.e., equilibrium partitioning) and proposed that the parameter that controls the position of x_{max} is the monomer volume fraction in the particles at equilibrium, ϕ.[44] Guo et al. used a kinetically limited partitioning of monomer and reported that microemulsion droplets disappear at 4% conversion but that the maximum reaction rate occurs at 20% conversion; they also found that the average number of free radicals per particle ($\tilde{n}$) is always smaller than 0.5 and decreases with conversion.[43] Evidently, even though microemulsion droplets disappear early in the reaction, the number of dead polymer particles swollen with monomer must be large enough (owing to the small value of $\tilde{n}$) to serve as monomer reservoirs that maintain the concentration of monomer at saturation to higher conversions. For VA and monomers with high solubility in water, particle generation at early stages of reaction must be dominated by homogeneous nucleation—although micellar nucleation may also contribute owing to the large initial number of microemulsion droplets. Microemulsion droplets and swollen dead polymer particles must supply monomer to maintain the monomer concentration constant in the increasing number of reacting particles. This should occur until the overall concentration of monomer is not enough to maintain monomer concentration at saturation in the aqueous phase and in the particles. However, more detailed experiments should be performed to explain the value of x_{max} and its invariance to reaction conditions.

R_{pmax} follows a power law with V-50 concentration with an exponent, α, equal to 0.8. Similar correlations between R_{pmax} and initiator concentration have been reported for the microemulsion polymerization of VA in CTAB microemulsions ($\alpha = 0.7$)[21] and in DDAB/DTAB microemulsions ($\alpha = 0.5$).[35] For the emulsion polymerization of VA, values of α equal to 0.64 and 0.7 have been reported for the reaction rate in the propagation stage.[45,46] These values,

(42) Mendizábal, E.; Flores, J.; Puig, J. E.; Katime, I.; López-Serrano, F.; Alvarez, J. *Macromol. Chem. Phys.*, in press.
(43) Guo, J. S.; Sudol, E. D.; Vanderhoff, J. W.; El-Aasser *J. Polym. Sci., Polym. Chem. Ed.* **1992**, *30*, 691.
(44) Mendizábal, E.; Flores, J.; Puig, J. E.; López-Serrano, F.; Alvarez, J. *Eur. Polym. J.* **1998**, *34*, 411.
(45) O'Donell, J. T.; Mesrobian, R. B.; Woodward, A. E. *J. Polym. Sci.* **1958**, *28*, 171.

which are larger than those predicted by the Smith−Ewart theory, can be attributed to the important contribution of homogeneous nucleation in the emulsion polymerization of this monomer.

Reaction rates and conversions obtained with KPS are higher than those achieved with V-50 (Figure 4). Since the concentrations of both initiators were chosen to produce the same flux of free radicals, kinetic differences can only be explained by (i) pH artifacts and (ii) electrostatic interactions. The decomposition rate constant of KPS varies with pH,[47] whereas that of V-50 does not appear to depend on pH.[36] For the polymerization rate of VA in AOT microemulsions initiated with KPS, the fastest reaction rate was achieved at a pH of 7.[36] Data shown in Figure 4 were obtained with a buffer to maintain the pH at a value of 7, so pH artifacts can be ruled out. Notice that the reaction rate with KPS is similar to that produced with V-50 at equal concentrations (cf. Figures 2 and 4) even though the latter is producing 10 times more radicals per unit time. Here we propose that the negatively charged microemulsion droplets "trap" cationic free radicals of V-50 and reduce their efficiency to initiate the reaction. By contrast, the negatively charged KPS free radicals are repelled by the droplets into the aqueous phase where they can react with the monomer dissolved there. These oligomeric radicals can grow up to a critical size and enter microemulsion droplets and existing particles or can be stabilized by recruiting surfactant and grow to become particles.

R_{pmax} follows an Arrhenius behavior with an activation energy (82 kJ/mol) that is larger than those reported for the polymerization of VA in CTAB microemulsions (69 kJ/mol)[22] and in DTAB/DDAB microemulsions (64 kJ/mol),[35] both also initiated with V-50. Inasmuch as reaction rates are faster in the latter systems,[21,35] the differences in activation energies (and reaction rates) can be a consequence of the different electrostatic interactions existing in these systems, as discussed above. In the CTAB and the DTAB/DDAB systems, interactions between the cationic free radicals of V-50 and the cationic droplets are repulsive, whereas in the AOT system, the interactions between the V-50 radicals and the anionic AOT droplets are attractive. Hence, the "electrostatic cage effect"[48] becomes operative in the latter system yielding slower reaction rates and a higher activation energy than in the CTAB and DTAB/DDAB systems.

The polymerization of VA in emulsions stabilized with AOT is faster and yields higher conversions with both KPS and V-50 than their counterparts in microemulsion polymerization (cf. Figures 4A and 5A) because of the higher monomer and initiator concentrations employed (three times larger), so it is not possible to compare absolute reaction rates. Nevertheless, three distinct reaction rates can be detected (Figure 5B) in contrast to microemulsion polymerization, where only two stages are seen (Figures 2B, 3B, and 4B). The constant reaction rate in the propagation stage is significantly faster than the R_{pmax} of the microemulsion polymerization. Furthermore, the evolution of $\bar{M}_n$ and $\bar{M}_w/\bar{M}_n$ with conversion in emulsion polymerization (Table 6) is notoriously different from that in microemulsion polymerization (Table 5).

In the batch emulsion polymerization of this monomer, termination reactions at low conversions are mainly due to chain transfer to monomer, which yields values of $\bar{M}_n$ around $(3-5) \times 10^5$ g/mol and a low $\bar{M}_w/\bar{M}_n$ ($\approx$2) whereas at higher conversions ($\geq$30−40%), chain transfer to polymer and terminal double-bond reactions produce branched polymers of high molar mass, which lead to a high $\bar{M}_w/\bar{M}_n$.[23−26] These effects are particularly severe at high conversions, where the reacting particles contain a high number density of macromolecules. Data for the polymerization of VA in AOT emulsions show these trends: values of $\bar{M}_n$ around 5×10^5 and low $\bar{M}_w/\bar{M}_n$ at low conversions and increasingly larger values of these parameters as the reaction proceeds (Table 6).

Inasmuch as $\bar{M}_n$ and $\bar{M}_w/\bar{M}_n$ are about the same at all conversions for microemulsion polymerization (Table 5) and since $\bar{M}_n$ and $\bar{M}_w/\bar{M}_n$ for the emulsion and microemulsion polymerizations examined here are similar at low conversions (cf. Tables 5 and 6), this leads us to suspect that chain transfer to monomer is the controlling termination mechanism for the polymerization of VA in AOT microemulsions.

For a 0−1 reacting system dominated by chain transfer to monomer, the number average molar mass is given by[49]

$$\bar{M}_n = \left(\frac{k_p}{k_{tr,M}}\right) M_0$$

For VA, the rate constant for chain transfer to monomer, $k_{tr,M}$, is $4.03-6.44 \times 10^{-4}$ $m^3 \cdot mol^{-1} \cdot s^{-1}$ at 60 °C[49] and k_p is 2.3 $m^3 \cdot mol^{-1} \cdot s^{-1}$ at the same temperature.[39] With these values, $\bar{M}_n$ was estimated to be $(3.1-4.9) \times 10^5$ g/mol. Inasmuch as the number-average molar masses obtained in this work (Tables 3−5) clearly fall within this theoretical range, this indicates that chain-transfer reactions to monomer control chain termination in the polymerization of VA in AOT microemulsions during the *whole* reaction. Moreover, the values of $\bar{M}_w/\bar{M}_n$ are also within the expected range of termination owing to chain transfer to monomer. Likewise, the values of $\bar{M}_n$ for the polymerization in emulsions stabilized with AOT at low conversions are within the theoretical range of termination by chain-transfer reactions to monomer; at higher conversions, evidently, chain transfer to polymer and, perhaps, terminal double-bond reactions dominate chain growth and termination events.

To show conclusively that chain transfer to monomer is the controlling termination mechanism from low to high conversions in microemulsion polymerization, the whole molar mass distributions (MMD) obtained by GPC were analyzed as a function of initiator concentration. The plot of the logarithm of the instantaneous number MMD, log $P(M)$, versus molar mass should give a straight line when chain transfer to monomer is the controlling mechanism.[2] Our GPC data plotted as log $P(M)$ versus M are linear for all V-50 concentrations (correlation coefficient better than 0.994 in all cases) with similar slopes (Figure 6), which completely demonstrates that chain transfer to monomer is *indeed* the governing termination mechanism at all conversions. From the slope of such plots, the values of $k_{tr,M}$ were estimated for the polymerizations initiated with the various V-50 concentrations, yielding an average value of 6.4×10^{-4} $m^3 \cdot mol^{-1} \cdot s^{-1}$, which is within the range reported for $k_{tr,M}$ of VA at 60 °C.[49]

Particle size appears to be the key factor in the distinct termination mechanisms observed here for emulsion and microemulsion polymerization. Owing to differences in size, the probability that a radical formed by chain transfer to monomer can escape from microemulsion-made par-

(46) Dunn, A. S.; Taylor, P. A. *Makromol. Chem.* **1965**, *83*, 207.
(47) Behrman, E. L.; Edwards, J. O. *Rev. Inorg. Chem.* **1980**, *2*, 179.
(48) Friend, J. P.; Alexander, A. E. *J. Polym. Sci., Polym. Chem. Ed.* **1968**, *16*, 1833.
(49) Odian, G. *Principles of Polymerization*; Wiley: New York, 1991.

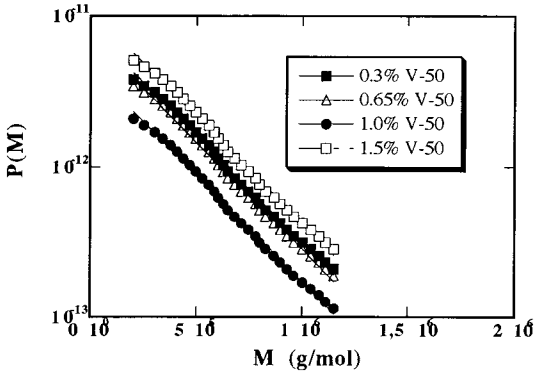

Figure 6. Logarithm of the instantaneous number-average MMD, $P(M)$, versus molar mass, M, for poly(vinyl acetate) as a function of the concentration of V-50 used in the polymerization. Samples at final conversions reported in Figure 2 were used.

ticles (25−30 nm) is larger than that from emulsion-made particles (80−100 nm). In fact, Guo et al. found much higher desorption rate constants in the microemulsion polymerization of styrene than in emulsion polymerization.[28] For various monomers, Mendizábal et al. also reported much higher desorption rate constants in microemulsion polymerization.[42,44] Moreover, the average number of chains per particle is much smaller in microemulsion polymerization, even at high conversion. This fact may also contribute to diminish the probability of chain transfer to polymer at high conversions.

Our hypothesis is supported by data reported elsewhere. In the polymerization of VA in CTAB or DTAB/DDAB microemulsions, bimodal (low and high) MMD were obtained.[22,35] In the former case, smaller particles (35−50 nm) and mostly low MMD polymer (with $\bar{M}_n$ values in the range of the theoretical ones for chain transfer to monomer) were obtained, whereas in the latter case, larger particles (70−100 nm) and mostly high MMD polymer were produced.

The results reported here demonstrate that emulsion and microemulsion polymerization processes are *indeed* different. Not only do they exhibit different kinetics and mechanisms but also the polymers produced are, in some cases, structurally different. It appears that for the polymerization of VA in microemulsions stabilized with Aerosol OT, the main controlling mechanism of chain growth and termination is chain-transfer reactions to monomer at all conversions. This unusual free radical polymerization behavior is apparently caused by the smaller particle size and the small average number of polymer chains per particle, which allows fast desorption rates of the monomeric radicals. To prove conclusively that chain transfer to monomer and not to polymer controls the MMD and that the poly(vinyl acetate) produced here contains a small degree of branching, even at high conversions, ^{13}C NMR analysis are underway, following the method reported by Britton and collaborators.[50]

Acknowledgment. This work was supported by CONACYT (Grant 3312). One of us (J.E.P.) acknowledges the visiting professor position granted by the Government of the Basque Country.

LA991065M

(50) Britton, D.; Heatley, F.; Lovell, P. A. *Macromolecules* **1998**, *31*, 2828.